Atmos. Chem. Phys. Discuss., 9, 22103–22141, 2009
www.atmos-chem-phys-discuss.net/9/22103/2009/


Atmospheric Chemistry and Physics Discussions

This discussion paper is/has been under review for the journal *Atmospheric Chemistry and Physics (ACP)*. Please refer to the corresponding final paper in *ACP* if available.

# Impact of open crop residual burning on air quality over Central Eastern China during the Mount Tai Experiment 2006 (MTX2006)

**K. Yamaji[1], J. Li[1,5], I. Uno[1,2], Y. Kanaya[1], Y. Komazaki[1], P. Pochanart[1], Y. Liu[1,5], M. Takigawa[1], T. Ohara[3], X. Yan[4], Z. Wang[5], and H. Akimoto[1,6]**

[1]Japan Agency for Marine-Earth Science and Technology, 3173-25, Showa-machi, Yokohama, Kanagawa 236-0001, Japan
[2]Research Institute for Applied Mechanics, Kyushu University, Kasuga Park 6-1, Kasuga 816-8580, Fukuoka, Japan
[3]National Institute for Environmental Studies, 16-2, Onogawa, Tsukuba, Ibaraki 305-8506, Japan





[4] Institute of Soil Science Chinese Academy of Sciences, Nanjing 210008, China
[5] Institute of Atmospheric Physics, Chinese Academy of Sciences, Beijing 10029, China
[6] Acid Deposition and Oxidant Research Center, 1182 Sowa, Nishi-ku, Niigata, Japan

Received: 29 September 2009 – Accepted: 5 October 2009 – Published: 21 October 2009

Correspondence to: K. Yamaji (kazuyo@jamstec.go.jp)

Published by Copernicus Publications on behalf of the European Geosciences Union.





## Abstract

The impact of open crop residual burning on $O_3$, CO, Black Carbons (BC), and Organic Carbons (OC) concentrations over Central Eastern China (CEC) during the Mount Tai Experiment 2006 (MTX2006) was evaluated using the regional chemical transport model, the Models-3 Community Multiscale Air Quality Modeling System (CMAQ). To investigate these pollutants during the MTX2006 period in June, daily gridded emissions from open crop residual burning were developed based on a bottom-up methodology and using land cover and hotspot information from satellites. This model system which involves daily emissions from open biomass burning, captured monthly-averaged observed concentrations and day-to-day variations in the patterns of $O_3$, CO, BC, and OC with good correlation coefficients between models and observations, ranging from 0.54 to 0.66. These results were significantly improved from those using annual emissions. For monthly-averaged $O_3$, the simulated concentration of 81.5 ppbv was close to the observed concentration (82.5 ppbv). The period of MTX2006 was roughly divided into two parts: 1) polluted days with heavy open crop residual burning in the first half of June; 2) cleaner days with negligible field burning in the latter half of June. Additionally, the first half of June was defined by two high pollution episodes during 5–7 and 12–13 June, and a relatively cleaner episode during 8–10 June between these two high pollution episodes. In the first polluted episode, this model captured high $O_3$, CO, BC, and OC concentrations at the summit of Mount Tai which were affected by open crop residual burning in the south of CEC and northward transport. For this episode, the impacts from open crop residual burning were 12% for $O_3$, 35% for CO, 56% for BC, and 80% for OC over CEC. The daily emissions from open crop residual burning were an essential factor to evaluate the pollutants during the MTX2006. These emissions have a large impact not only on primary pollutants but also on secondly pollutions, such as $O_3$, in the first half of June over northeastern Asia. On the other hand, this model did not capture the second polluted episode and underestimated observed CO and BC. Improvements of both anthropogenic and open burning emissions and CO inflow



ACPD

9, 22103–22141, 2009



from model boundary are necessary to improve both anthropogenic and open burning emissions and CO inflow to evaluate the pollutants using this model.

## 1 Introduction

Central Eastern China (CEC) (Fig. 1) has received attention as a region containing trace gases and aerosol pollutants, which are causative agents of serious air pollution and important components contributing to global radiation budgets. Bottom-up emission estimation studies (e.g. Olivier et al., 1999; Streets et al., 2003; Ohara et al., 2007) have shown that CEC is a largest emission source for anthropogenic sectors. He et al. (2008) performed long-term air pollutant observations and a modeling study at three mountain tops, Mount Tai (36.25° N, 117.10° E, 1533 m a.s.l.), Mount Hua (34.49° N, 110.09° E, 2064 m a.s.l.), and Mount Huang (30.13° N, 118.15° E, 1836 m a.s.l.) located in or near CEC (Fig. 1). Several MTX2006-related papers have indicated that monthly-averaged $O_3$ peaks usually appear in June, with more than 60 ppbv, and the maximum hourly $O_3$ reached was 150 ppbv in each year of 2004–2006 (Li et al., 2007; He et al., 2008). In particular, the monthly-averaged $O_3$ at the summit of Mount Tai exceeded 80 ppbv in June. Gao et al. (2005) based on mid-term observations in July–November 2003, indicated that monthly-averaged $O_3$ and CO peaks appeared in July with values of 65 and 439 ppbv, respectively. Several regional modeling studies (Li et al., 2007; He et al., 2008; Yamaji et al., 2008) captured this seasonal cycle which peaked in early summer (June–July), but systematically failed to simulate such high concentrations. These underestimates seemed to be caused by rapid increases in anthropogenic emissions after 2000, in addition to uncertainties in the temporal and spatial distributions of agricultural waste burning, and an insufficient grid resolution to reproduce meteorological fields at an isolated mountain surrounded by high emission sources (Yamaji et al., 2008).

Recently, tropospheric satellite observations have demonstrated that emissions of the major $O_3$ precursor, $NO_x$, in CEC have accelerated since 2000 (Richter et al., 2005;



ACPD
9, 22103–22141, 2009



Irie et al., 2005, 2009). Richter et al. (2005) found a highly significant increase over the industrial area of China (same area as CEC) which was more than that demonstrated in a bottom-up inventory by Streets et al. (2000). Even during 1998–2000, Uno et al. (2007) found that GOME-satellite $NO_2$ was increased more than the simulated $NO_2$ using the Models-3 Community Multiscale Air Quality Modeling System (CMAQ) with a bottom-up inventory, (Regional emission inventory in Asia (REAS), Ohara et al., 2007). Many recent studies have indicated that significant uncertainties may exist in most emission inventories for pollutants from Asia in general and from East Asia in particular, especially for CO (e.g. Kasibhatla et al., 2002; Pétron et al., 2002; Kiley et al., 2003; Palmer et al., 2003; Carmichael et al., 2003; Arellano et al., 2004; Allen et al., 2004; Tan et al., 2004). A modeling study using the Regional Acid Deposition Model (RADM) with the ACE-Asia and TRACE-P Modeling and Emission Support System (ACESS) (Streets et al., 2003) for Lin'an (30° N, 119° E, 132 m a.s.l.) suggested that a 50% increase in emission would bring the model-calculated concentrations into agreement with observations (Tan et al., 2004). Subsequently, Streets et al. (2006) showed that China's CO emission was 157 Tg $yr^{-1}$ in 2001, which was 36% higher than the ACESS estimate (116 Tg $yr^{-1}$) for the year 2000 (Streets et al., 2003).

As part of an intensive field observation campaign, the Mount Tai Experiment 2006 (MTX2006) was carried out to evaluate the emission source, tropospheric chemistry, transformation, and transport of atmospheric pollutants, $O_3$, aerosols, and their precursors over CEC in June 2006. As mentioned in Kanaya et al. (2008) and Li et al. (2008a), high polluted episodes (5–7 June and 11–13 June) are clearly shown in Fig. 2, conditions e–h, particularly for Black Carbons (BC) or Elemental Carbons (EC) and Organic Carbons (OC). In addition, $O_3$ and CO during these polluted episodes were relatively high compared with the cleaner days (8–10 June) between the two polluted episodes, however, they were not the highest in June (Fig. 2, conditions e–h). In our previous study for the year 2000, simulated $O_3$ reproduced well the seasonal variations in the observed values at Japanese remote sites, but the monthly-averaged $O_3$ was underestimated by 5–15 ppbv at Mount Tai in June (Yamaji et al., 2008). As indicated in



ACPD
9, 22103–22141, 2009



Fig. 2, conditions e–h, all simulated pollutants ($O_3$, CO, EC, and OC) for the MTX2006 were underestimated based on a sensitivity model experimental design, R00AAD in Table 1, which was the same as that in our previous study (Yamaji et al., 2008). The simulated monthly-averaged $O_3$ was underestimated by 12.4 ppbv, which was similar to our previous findings (Yamaji et al., 2008). The simulated monthly-averaged CO was much lower than the observed concentration by a factor of around 3. As for BC and OC, although the concentration levels were captured by this model for the latter half of June during the cleaner days (Kanaya et al., 2008; Li et al., 2008a), the model failed to reproduce the high polluted episodes (5–7 June and 11–13 June).

Several studies on this issue have suggested that the high polluted episodes (5–7 June and 11–13 June) likely stemmed from significant open biomass burning of agricultural crop residue (Kanaya et al., 2008; Li et al., 2008a). In fact, as shown in Fig. 3, a large number of hotspots were detected by Aqua/Terra MODIS (MOderate resolution Imaging Spectroradiometer, http://webmodis.iis.u-tokyo.ac.jp/) over the southern part of the North China Plain (south of Mount Tai) in the first ten days of June (1–10 June). During the next ten days (11–20 June), hotspot intensities were found in some parts of the North China Plain. However, a few hotspots were detected over China (southern China) during 21–30 June. These fire events seemed to be strongly associated with agricultural waste burning in the field after the wheat harvest and was also reported by the State Environmental Protection Administration (SEPA) in China (http://www.sepa.gov.cn). Therefore, a cause for the underestimation in this model appears to come from the limited temporal emission inventory from crop residue burning in the field such as the annual emission inventory. In addition, we found that the emission spatial intensities using the ACESS inventory for biomass burning (Streets et al., 2003) did not necessarily correspond to the hotspot positions for the year 2006, with a focus on different months of the year. Even in their revision of the ACESS inventory, Streets et al. (2006) admitted to an uncertainty about the magnitude of CO emissions from the burning of crop residues in the field.

In this study, the impact of open crop residual burning on regional $O_3$, CO, BC (sim-



ACPD
9, 22103–22141, 2009



ulated EC), and OC fields was examined using a regional chemical transport model (CTM), which involved daily biomass burning emissions during the MTX2006. In the following section (Sect. 2), we describe the emission inventory used in this study, with a focus on daily gridded emissions from open crop residual burning in China. The representation of a regional CTM and the sensitivity model experimental design are discussed in Sect. 3. We report the results of day-by-day variations in pollutants at the summit of Mount Tai and their special distributions over northeast Asia based on the regional CTM using daily emissions from open crop residual burning in Sect. 4.

## 2 Emission inventories

### 2.1 Annual and monthly emissions estimation

#### 2.1.1 Emissions from open crop residual burning in China

After harvest, crop residue is either directly returned to agriculture fields as fertilizer, burned in the field, or used as biofuel. However, it is difficult to obtain accurate amounts for the management of these crop residues because of the lack of relevant statistical data. Gao et al. (2002) prepared a crop residue balance sheet for 21 provinces in China based on extensive survey data, in which only 6.6% of the crop residue was burned in the field, and on average 36.6% of the crop residue was directly returned to the soil. However, most other experts estimated around 15–20% of crop residues were directly returned to the soil (e.g., Yang, 1994; Song, 1995; MOA/DOE Project Expert Team, 1998; Li, 2003). The percentages calculated by Gao et al. (2002) for crop residue returned to the soil were overestimated by 16.6–21.6%. Therefore, Yan et al. (2006) recommended adding 16.6% to the percentage for each province. However, this adjustment was not applied to some provinces where more than 30% of the crop residue was burned in the field (Gao et al., 2002). For the other provinces not listed in the study by Gao et al. (2002), the percentages in the neighboring province with



ACPD
9, 22103–22141, 2009



similar conditions or the national average (19.4%) were used. We used the adjustment percentages recommended by Yan et al. (2006) in this study. In particular, for several provinces surrounding Mount Tai, we employed the following percentages: 19.6% (Shandong), 17.5% (Anhui), 22.4% (Henan), 11.3% (Hebei), and 33.9% (Jiangsu). The residue amounts for major crops were obtained from the grain amount (Editorial Board of China Agricultural Statistical Yearbook (EBCASY), 2007) and the residue/grain ratio (Yan et al., 2006). The emission factors from Andreae and Merlet (2001) were used, which were also cited by the other inventories (e.g. Streets et al., 2003; Yan et al., 2006).

For annual emissions from open crop residual burning in each province, we employed a bottom-up methodology by Yan et al. (2006), in which the emissions for the year 2000 were estimated from biomass consumption and emission factors. Annual emissions ($NO_x$, $SO_2$, CO, $NH_3$, EC, OC, and NMVOC) from open crop residual burning in China for the year 2006 were updated from Yan et al. (2006). All species increased by roughly 13% for 2000–2006, and was caused by an agricultural production increase (Table 2). In some provinces (Helongjian, Jinlin, Liaoning, Inner Mongolia, Ningxia, Shanxi, and Tianjing), the emissions increased by more than 30% during this period. Shandong province where Mount Tai is located and its nearby provinces with the exception of Jiangsu (Hebei, Henan, and Anhui) had increases of 8–28% during 2000–2006. In the other cities and provinces (Beijing, Chongqing, Guangdong, Guizhou, Hainan, Hunan, Jiangsu, Shanghai, Sichuan, and Zhejiang), the emissions decreased by a few percent up to 50%. As for the open crop residual burning in China used in these model experiments, the annual emissions accounted for 66% ($NO_x$), 51% ($SO_2$), 69% (CO), 70% ($NH_3$), 75% (EC), 48% (OC), and 65% (NMVOC) of Chinese emissions from total open biomass burning.

As shown in Table 2, estimated emissions from Chinese open crop residual burning by Yan et al. (2006) were larger than those of the ACESS inventory (Streets et al., 2003) by ≈16%, which was mainly caused by a difference in the estimated amounts of burned dry matter in the field. The differences between Yan et al. (2006) and the



ACPD
9, 22103–22141, 2009



ACESS inventory (Streets et al., 2003) for forest and grassland fires were also caused by estimated amounts of burned biomass.

### 2.1.2 Emission from forest and grassland burning

Yan et al. (2006) estimated pollutions emissions from forest and grassland fires in China based on both satellite data and statistics. They showed large discrepancies between satellite data and statistics; estimated amounts of burned biomass were 50.8 (satellite) and 2.1 (statistics) Tg dry matter $yr^{-1}$ for forest fires: 5.5 (satellite) and 0.2 (statistics) Tg dry matter $yr^{-1}$ for grassland fires (Yan et al., 2006). On the other hand, Streets et al. (2003) found amounts of burned biomass of 25 Tg dry matter $yr^{-1}$ for forest fires and 52 Tg dry matter $yr^{-1}$ for grassland fires in China, which was obtained by using fire statistical data for 1950–1992. It was shown that there were still large discrepancies between the amounts of burned biomass using different methodologies (Yan et al., 2006). For this simulation, the estimated emissions from forest and grassland fires based on satellite data by Yan et al. (2006) were used. Annual emissions from biomass burning in Asia, with the exception of China, were obtained from the ACESS final version (Streets et al., 2003).

### 2.1.3 Anthropogenic emissions

Annual atmospheric pollutants emissions ($NO_x$, $SO_2$, CO, $NH_3$, EC, OC, and NMVOC) from anthropogenic sources excluding biomass combustion in the field (fuel combustion, non-combustion industry, agriculture, and domestic activities) were based on the Regional Emission inventory in ASia (REAS) (Yan et al., 2003; Yamaji et al., 2003; Yamaji et al., 2004; Ohara et al., 2007), which is available from http://www.jamstec.go.jp/frcgc/research/p3/emission.htm. REAS, a bottom-up regional emission inventory for Asia with a 0.5° spatial resolution, provides a sequence of gridded emission data from the past (from 1980 to 2003) to the future (2010 and 2020) based on three emission scenarios, the reference (REF), the policy succeed case (PSC), and the pol-



ACPD
9, 22103–22141, 2009



icy failure case (PFC) scenarios. The future emissions predictions are based on the emissions in 2000 (Ohara et al., 2007). The PFC scenario may be more plausible when judged according to the recent trend in anthropogenic $NO_x$ emissions in China after the year 2000, which increased from 11.2 in 2000 to 14.5 $Tg\,yr^{-1}$ in 2003, as reported by Akimoto et al. (2006) and Ohara et al. (2007). For this model study, therefore, the emissions data in the year 2006 were obtained by simple interpolation using the amounts in 2003 and 2010 (PFC). The ACESS data are available at http://www.cgrer.uiowa.edu/ACESS/acess_index.htm.

#### 2.1.4 Natural emissions

Biogenic NMVOC emissions, isoprene and terpene were obtained from the Global Emission Inventory Activity (GEIA) $1^{\circ}\times1^{\circ}$ monthly global inventory (Guenther et al., 1995). We employed the temporal and spatial distributions for these emissions from original databases in this study. Emissions from natural sources, e.g., soil and lightning $NO_x$ were not considered in our model simulations.

#### 2.1.5 Daily gridded emissions

As for the causes, locations, and timing, open biomass burning (field burning of crop residue and forest and grassland fires) is different from the other anthropogenic sources (e.g. fuel combustion and non-combustion industry), and thus annual pollutants emissions from open biomass burning cannot be allocated over time and space in the same way as the other anthropogenic sources. The field burning of crop residue is strongly correlated with agriculture practices, and forest and grassland fires are caused by both natural and human accidents (Streets et al., 2003). As mentioned in the section above, the emissions inventory for open biomass burning with correct spatial and temporal distributions is needed to simulate the behavior of atmospheric pollutants in CEC in June. Therefore, for this simulation we tried to allocate the annual emissions from open biomass burning (field burning of crop residue and forest and



ACPD
9, 22103–22141, 2009



grassland burning) for country and Chinese province levels into daily gridded data with a 0.5° resolution based on satellite hotspots, the area of the province and land cover gridded information. The Aqua/Terra MODIS provided more available data for June 2006 than the NOAA AVHRR and ESA ATSR, therefore, Asian daily hotspot maps with a 1 km resolution, which are based on the MODIS fire database and available at http://webmodis.iis.u-tokyo.ac.jp, were employed in this study. However, the MODIS fire data still included irregular no-fire days between large fire events. To avoid unusual concentrations over a few days, this study used the fire data normalized using data for 5 days. Additionally, the Gridded Population of the World version 2 dataset (available at http://sedac.ciesin.org) and the AARS Asia 30-second Land Cover Data Set with Ground Truth Information giving the land cover gridded database (available at http://www.cr.chiba-u.jp) were used to detect the burned area, country or province, and land cover type.

The selected emission maps, $NO_x$, CO, Primary Elemental Carbons (PEC), and POC from all emission sources on 7, 10, 12, and 28 June 2006 are shown in Fig. 4. During the first half of June 2006, large numbers of fire spots were detected over the southern part of CEC and were placed to the south of Mount Tai by some satellite sensors, e.g. Aqua/Terra MODIS, NOAA AVHRR, and ESA ATSR. For this period, as shown in Fig. 4, on 7, 10, and 12 June 2006, high $NO_x$, CO, PEC, and POC emissions were detected over the south part of the North China Plain. In particular, for 7 June 2006, $NO_{CEC was highest in June x}$ and CO emission over CEC was highest in June (Fig. 2, condition c, d) and the highest $NO_x$, CO, PEC, and POC emission flux per grid reached 450 mol $s^{-1}$ $grid^{-1}$, 17 600 mol $s^{-1}$ $grid^{-1}$, 3720 g $s^{-1}$ $grid^{-1}$, and 16 500 g $s^{-1}$ $grid^{-1}$, respectively. Meanwhile, a few fire spots were detected over China during the latter half of June as shown in Fig. 3. Such high emissions caused by open biomass burning during the first half of June were not found over China on 28 June (Fig. 4). Moreover, even for annual emissions at the province level and the annual emissions distribution pattern over CEC, these gridded emissions of open biomass burning for the year 2006 gave different distribution patterns, when compared to those for the year 2001 (Streets



ACPD
9, 22103–22141, 2009



et al., 2003).

For open crop residual burning over CEC, ≈40% of annual emissions were detected in June. The open crop residual burning on 7 June was about 14% of the monthly total (about 6% of the annual total). Figure 2c and d show the daily $NO_x$ and CO emission flux from CEC in June, respectively. The impact of crop residual open burning was considerably high during 6–9 June. The contributions were 31.4–44.3% ($NO_x$) and 47.0–60.5% (CO) of the total sources. The largest appeared on 7 June. The impact was reduced by ≈10–20% (but not to zero) on 11–12 June, and then increased again and reached 27.5% ($NO_x$) and 39.2% (CO) on 14 June. After 20 June, the impact of open crop residual burning was almost zero, and daily total $NO_x$ and CO emission flux did not show a day-to-day variation.

## 3 Regional chemical transport model system and sensitivity experiment design

The modeling system employed in this study was CMAQ version 4.4 (Byun and Ching, 1999) driven by the meteorological fields calculated by the Regional Atmospheric Modeling System (RAMS) Version 4.4 (Pielke et al., 1992; Cotton et al., 2003). This RAMS simulation used the NCEP Global Tropospheric Analyses with a 1°×1° at 6-h intervals for the year 2006 data set. The off-line processor for combining CMAQ with RAMS was developed by Uno et al. (2007). Subsequently, Yamaji et al. (2006, 2008) evaluated simulated $O_3$ concentrations compared with observed $O_3$ at the Sea of Japan region provided by the Acid Deposition East Asia Monitoring Network (EANET) and World Data Centre for Greenhouse Gases (WDCGG), and Mount Tai.

Spatial domains for CMAQ and RAMS shown in Fig. 1 are 6240×5440 $km^2$ (inside domain in Fig. 1) and 8000×5600 $km^2$ (outside domain in Fig. 1) on rotated polar stereographic map projections centered at 25° N and 115° E, respectively, with an 80×80 $km^2$ grid resolution. For the vertical resolution, both model systems have the same model height of 23 km and employ a hybrid sigma-pressure coordinate. CMAQ has 14 vertical layers, with about 7 layers below 2 km. RAMS has 23 vertical layers,



ACPD
9, 22103–22141, 2009



and about 7 layers within 2 km.

The CMAQ chemical-transport model (CCTM) requires information for the initial and boundary chemical concentrations. We used an initial condition to reflect chemical concentrations in East Asia; these conditions were applied to the CMAQ simulations by Zhang et al. (2002) and Yamaji et al. (2006, 2008). The boundary conditions of $O_3$ and its precursors, NO, $NO_2$, CO, ethane, and propane were obtained from daily averaged concentrations by the CHemical AGCM for Study of Atmospheric Environment and Radiative forcing, CHASER (Sudo et al., 2002; Sudo and Akimoto, 2007). The CCTM simulates the relevant and major atmospheric gas chemistry, transport, and deposition processes. As for the gas-phase atmospheric chemical mechanism, the Statewide Air Pollution Research Center (SAPRC)-99 (Carter, 2000), which has documented 72 chemical species and 214 chemical reactions, including 30 photochemical reactions, was employed with the mechanism-specific Euler Backward Iterative (EBI) solver. We also used the 3rd generation CMAQ aerosol module (AERO3), which includes SORGAM (Schell et al., 2001) as a secondary organic aerosol model, ISORROPIA (Nenes et al., 1998) as an inorganic aerosol model, and RPM (Binkowski and Shankar, 1995) as a regional particulate model.

This model simulation started on 1 May 2006. The first 1-month simulation is regarded as the spin-up and the following 1-month simulation was used for this analysis. The chemical concentrations used in this study are the instant CCTM outputs obtained every three hours starting at 00:00 UTC each day.

For sensitivity model experiments on emissions and boundary conditions, we employed five model designs as shown in Table 1: R06YDD using REAS for the year 2006, daily open biomass burning emissions for the year 2006, and daily boundary conditions from CHASER using emissions and meteorological conditions for the year 2006; R00AAM using REAS for the year 2000, annual biomass burning emissions for the year 2001 by Streets et al. (2003), and monthly-climate boundary conditions from CHASER using emissions and meteorological conditions for the 1990s; R00YDD using REAS for the year 2000, daily biomass burning emissions for the year 2006, and daily



ACPD
9, 22103–22141, 2009



boundary conditions for the year 2006; R06YAD using REAS for the year 2006, annual biomass burning emissions for the year 2006, and daily boundary conditions for the year 2006; R06YDM using REAS for the year 2006, daily biomass burning emissions for the year 2006, and monthly-climate boundary conditions.

## 4 Results and discussion

### 4.1 Comparison of simulated results and observations at the summit of Mount Tai

As mentioned in Li et al. (2008a), this observation campaign period was roughly divided into two parts: 1) polluted days with heavy field burning of crop residue in the first half of June; 2) cleaner days with negligible field burning in the latter half of June. Additionally, the first half of June was defined by two high pollution episodes during 5–7 and 12–13 June, and a relatively cleaner episode during 8–10 June between these two high pollution episodes. Wind directions and emissions from open crop residual burning south of Mount Tai will largely affect this pollution pattern. Therefore, in this section, after confirming reproducibility of the meteorological field mainly for wind pattern and water vapor in the air masses, we will discuss the simulated $O_3$, CO, EC, and OC concentrations at ≈1000-m altitude compared with the observed values. The detailed descriptions of these observations can be found in several MTX2006 related papers, e.g., gases ($O_3$ and CO) in Li et al. (2008a) and Kanaya et al. (2009) and BC or EC and OC in Kanaya et al. (2008). We will then discuss what affected these characteristic episodes, with a focus on both the impact of crop residue burning and meteorological conditions over CEC in subsequent sections.

Figure 2a illustrates daily-simulated and observed wind patterns at the summit of Mount Tai in June 2006. The daily-simulated wind direction and speed compared reasonably well with the meteorological observations. Figure 2b shows daily values of observed and simulated relative humidity (RH). In particular for early June, the high-



ACPD
9, 22103–22141, 2009



polluted episodes (5–7 and 12–13 June) were associated with a strong southwesterly wind and with relatively high humidity. The low-polluted period between these two peaks, on the other hand, was associated with a northwesterly wind with continental dry air masses. This model simulation successfully captured the characteristic exchange of these air masses, and therefore helped to predict the variation in atmospheric pollutants during polluted periods in this observational experiment. On the other hand, this model did not capture daily infrequently observed quick and large changes in wind direction. It should be noted that these changes could cause discrepancies between the simulated and observed concentrations of pollutants.

Figure 2e shows simulated daily $O_3$ concentrations for R06YDD and R00AAM, and observed $O_3$ concentrations. R06YDD roughly captured daily $O_3$ concentration levels and day-to-day $O_3$ variations with a correlation coefficient of 0.61 between the model and the observations. These results were much better than those obtained ($r$=0.48) by R00AAM (Table 3). In particular, for early June, simulated $O_3$ which considered daily emissions from open crop residual burning, successfully captured the high value of more than 100 ppbv of daily $O_3$. Subsequently, for 8–10 June, relatively low $O_3$ was also successfully simulated because this meteorological model captured the change in wind direction from southwesterly to northwesterly. On the other hand, this model tended to underestimate observed $O_3$ for the second high-polluted episode (12–13 June). The simulated $O_3$ peak seemed to be one day behind that of the observed peak on 12 June. This one-day delay in the second high-polluted episode was also shown by Li et al. (2008), and was caused by the temporal distribution of emissions which peaked on 14 June. During 20–25 June, daily-averaged $O_3$ by both R06YDD and R00AAM seemed to be reasonable. The simulated monthly $O_3$ concentration (81.5 ppbv) was comparable to the observed concentration (82.5 ppbv). This result with R06YDD seemed to be better than that with R00AAM which underestimated by around 5–15 ppbv during June (Yamaji et al., 2008), because this model experiment used updated anthropogenic emissions (energy and open crop residual burning in China) considering recent economic growth during 2000–2006 in China, and consid-



ACPD
9, 22103–22141, 2009



ered in detail spatial and temporal distributions of emissions from open crop residual burning over China coupled with satellite hotspot data.

This model tended to underestimate observed CO during the whole experimental period, although the simulated day-to-day variation pattern was reasonable compared to the observed pattern with a correlation coefficient of 0.54 (Fig. 2f and Table 3). CO was distinctive in that the simulated concentrations were less than the observed concentrations by around 150–500 ppbv for the daily average even in the latter half of June, when less biomass was burned as mentioned by Kanaya et al. (2008) and Li et al. (2008a). This suggests underestimates of CO emissions from energy sectors and/or CO inflow from this model boundary. As a result, monthly-averaged CO concentration (313.1 ppbv) by the model was much lower than the observation (567.7 ppbv). The previous observation campaign base studies in east Asia suggested that the ACESS inventory (Street et al., 2003), especially for Chinese CO emission was also underestimated by around 50% (e.g. Carmichael et al., 2003; Palmer et al., 2003; Wang et al., 2004; Tan et al., 2004). Carmichael et al. (2003) indicated that the domestic sector would have to be increased by 3–5 times to reconcile the model results for CO with the observations. On the basis of these results, Street et al. (2006) revised China's CO to be 157 Tg in 2001 which was 36% higher than the previous estimation for the year 2000 of 116 Tg (Street et al., 2003), and indicated that estimations of CO from China should be in the order of 140–200 Tg $yr^{-1}$. Our anthropogenic emission inventory with 141 Tg $yr^{-1}$CO from China in 2001 (Ohara et al., 2007) might still be an underestimate. As mentioned for $O_3$, the second concentration peak in simulated CO also appeared on 14 June, and was one day behind the observed concentration, and was affected by the temporal distribution of emissions (Fig. 2f). In addition, discrepancies between the simulated and observed second concentration peak were found in $O_3$, BC, and OC. These findings suggest that the temporal distribution of emissions from open crop residual burning still needs improvement. Even baseline CO concentrations were underestimated by the model, and that mean that the inflow of CO from the boundary was already under-simulated, although underestimation of the high CO events might



ACPD
9, 22103–22141, 2009



be caused by both regional emissions from open biomass burning and from other anthropogenic sources.

Mass concentrations of BC (or EC) were determined using four instruments, an ECOC semi-continuous analyzer (Sunset Laboratory), a multi-angle absorption photometer (5012 MAAP, Thermo), a particle soot absorption photometer (PSAP, Radiance Research), and an Aethalometer (AE-21, Magge Scientific) in the MTX2006 (Kanaya et al., 2009). At the same time, mass concentrations of OC were determined by the ECOC analyzer. The differences between these instruments were discussed in detail in Kanaya et al. (2009). The general magnitude relationship was shown to be EC (PM1, NIOSI) ~ opt-EC (PM1) < heated PSAP_BC (PM1) ~ MAAP_BC (PM1), and the largest discrepancy was found between EC (PM1, NIOSI) and MAAP_BC (PM1), with a slope of 1.41. In Fig. 2g, simulated daily EC concentrations were compared with both the highest values using the ECOC analyzers and the lowest values using the MAAP analyzers. Figure 2h shows the daily concentrations of simulated and observed OC. It should be noted that secondary organic molecules (SOMs) were included in simulated OC. Although a factor of 1.2–1.4 for estimating average organic molecular weight per carbon weight (White and Roberts, 1977) or 1.6 for urban aerosol (Turpin and Lim, 2001) should technically be considered for SOM, we ignored the factor in this study. Observed BC (or EC) and OC concentrations using the ECOC analyzer and the MAAP analyzer which had similar day-to-day variation patterns were successfully captured by model R06YDD, with correlation coefficients of 0.63-0.66 and 0.63, respectively (Fig. 2g and h and Table 3). For the high-polluted peaks in early June, as shown in Fig. 2g and h, R06YDD was better than R00AAM. In particular for 7 June, simulated daily BC ($4\,\mu g\,m^{-3}$) and OC ($19\,\mu g\,m^{-3}$) concentrations by R06YDD were much closer to the observed values (7–$10\,\mu g\,C\,m^{-3}$ for BC or EC and $24\,\mu g\,C\,m^{-3}$ for OC) than those by R00AAM ($0.4\,\mu g\,m^{-3}$ for EC and $1\,\mu g\,m^{-3}$ for OC). For the daily averaged BC, however, even R06YDD still tended to underestimate by 20–60% compared to EC using the ECOC analyzer (30–80% for MAAP analyzer). For the second polluted peak during 12–13 June, as mentioned for $O_3$ and CO, reproducibility for BC



ACPD
9, 22103–22141, 2009



and OC concentrations probably due to open crop residual burning may still include the failure to capture pollution timing. This model simulated only 0.7–1.3 $\mu g\,m^{-3}$ for the daily averaged concentration of EC and did not capture the observed second peak of around 5–11 $\mu g\,C\,m^{-3}$. For the latter half of June, this model successfully simulated daily OC but tended to underestimate by more than a factor of 2 for BC. As for the monthly-averaged value, this model tended to underestimate by more than a factor of 2 for EC (ECOC analyzer), by 3.5 for BC (MAAP analyzer) and by 1.3 or more for OC (Table 3). These results suggest that BC emissions from both anthropogenic energy and open crop residual burning are still underestimated. This model also tended to underestimate OC, which may have been caused by underestimation of primary OC emission. However, it is suspected the secondary OC was also underestimated in this study, although this is unclear.

From the point of view of emissions, we suggest that daily gridded emissions from open biomass burning were efficient evaluating the atmospheric pollutants, $O_3$, CO, BC, and OC in the MTX2006. However, it is also suggested that more accurate emission information on estimated emission values from anthropogenic and open biomass burning and their daily emission distributions would help to simulate atmospheric pollutants over CEC. On the other hand, it should be noted that this model often failed to reproduce the diurnal variation in daytime pollution peaks associated with both the build-up of the planetary boundary layer (Kanaya et al., 2008) and the upslope motion of polluted air masses. In the former, this model which included 14 layers up to 23 km in altitude was possibly too coarse to simulate the observed build-up of the planetary boundary layer. In the latter, the horizontal resolution of this model was insufficient to reproduce an isolated mountain such as Mount Tai and cannot simulate observed air mass climbing. The monthly-averaged diurnal $O_3$ behavior was reproduced well using a regional CTM, with a fine horizontal resolution of 27 km and 20 layers by Li et al. (2008b), although this type of model has a limitation in that the horizontal resolution of 5 km can only reproduce an isolated mountain of around 500 m. It should be noted that this simulation used 80 km horizontal resolution, which was probably too coarse to re-



ACPD
9, 22103–22141, 2009



produce episodic polluted air masses. Therefore, simulated pollutants concentrations were attenuated in each model grid and underestimation of observations could not be avoided.

When R06YDD and R00AAM were compared, it was pointed out in the above sections that daily emissions of open biomass burning for the target year were absolutely necessary in reproducing the day-to-day variations and monthly concentrations of atmospheric pollutants for MTX2006. However, it is possible that the differences between these model experiments were caused by other reasons, e.g., anthropogenic emissions and boundary conditions. In order to demonstrate the merits of using daily emissions, 3 sensitivity model experiments were performed (see Table 1). Table 3 lists the comparisons between models and observations for the 5 model designs (Table 1). Efficient updating of anthropogenic emissions from 2000 to 2006 is found in R00YDD, including "REAS for the year 2000" and R06YDD, "REAS for the year 2006". For gases (CO and $O_3$), this update of anthropogenic emissions showed 5.7 ($O_3$) and 1.3 (CO) ppbv increases for the monthly average, because CO and ozone precursors increased during 2000–2006. R06YDD showed an $r$ of 0.61 ($O_3$) and 0.54 (CO) compared to R00YDD, which showed an $r$ ($O_3$)=0.68 and $r$ (CO)=0.49. For aerosols (BC or EC and OC), $r$ (0.63–0.66) for R06YDD was better than that for R00YDD ($r$=0.58–0.62), however, monthly concentrations by R06YDD reduced slightly which was caused by regional primary emission decreases. For the boundary conditions, direct differences between "daily CHASER" and "monthly-climate CHASER" were found when R06YDD was compared with R06YDM. With the exception of $O_3$, $r$ by R06YDD was better than that (0.46–0.62) by R06YDM. As for monthly-averaged concentrations, R06YDD caused a 3.6 ppbv increase in CO, a 3.2 ppbv decrease in $O_3$, and a few changes in aerosols. Comparing R06YDD with R06YAD showed the direct merit of using daily emissions from open biomass burning. R06YDD showed a 5.5 ($O_3$) ppbv, 71.5 (CO) ppbv, 0.5-0.7 $\mu g\,m^{-3}$ (EC), and 4.3 $\mu g\,m^{-3}$ (OC) increase compared with R06YAD. Although the increase in $O_3$ is the same level as that caused by anthropogenic emission changes from 2000–2006, the effect on monthly CO, EC, and OC concentrations of using daily



ACPD
9, 22103–22141, 2009



emissions was larger than the other modifications. Additionally, for $O_3$, EC, and OC, $r$ for R06YDD was much better than that for R06YAD ($r$=0.35 ($O_3$), 0.21–0.24 (EC), and 0.34 (OC)). There was no change in $r$ for CO. In the TRACE-P study, Heald et al. (2003) indicated that daily resolution of biomass burning emission was not critical for modeling outflow from tropical regions because they focused on correlation coefficients between observed and simulated CO over outflow regions. In this study which focused on source region, the daily emissions of open biomass burning benefit the modification of monthly-averaged concentrations and correlation coefficients on air pollutants simulations for MTX2006, although the daily emissions might not be critical for increments in correlation coefficients for CO.

### 4.2 Selected characteristic episodes at the Summit of Mount Tai

Daily atmospheric pollutants ($O_3$, CO, EC, and OC) distributions in near-ground, <1 km are shown in Fig. 5 with surface weather charts and wind patterns (<1 km) for each day in the selected characteristic episodes: Episode I-a, the first polluted peak on 7 June; Episode I-b, the second polluted peak on 12 June; Episode II, the relatively cleaner day on 10 June; Episode III, non-open crop residual burning on 28 June. In these episodes, $NO_x$, CO, PEC, and POC emissions in CEC and daily averaged atmospheric pollutants concentrations, $O_3$, CO, EC, and OC in CEC and at the summit of Mount Tai are listed in Table 4. The source regions attribution of $O_3$ with meteorological effects has been discussed in detail by Li e al. (2008a). In the current study, to focus on the impact of open crop residual burning, the contributions from the differences between R06YDD and the other simulation without emissions from open crop residual burning were calculated and are shown as percentages in Fig. 5 and Table 3.

#### 4.2.1 Observed polluted peaks, Episode I-a and Episode I-b

Both observed polluted peaks on 7 and 12 June (Episode I-a and Episode I-b, respectively) were under similar meteorological conditions controlled by northward and



ACPD
9, 22103–22141, 2009



northeastward transport toward a strong low pressure located in northeastern China, particularly in and around the east coastal area of CEC (Fig. 5 Episode I-a and I-b). The strong low pressure stayed just north of the Mount Tai, therefore these observed high-polluted episodes at the summit of Mount Tai were probably affected by wind from the south of CEC. In particular, for 7 June, this model captured the polluted episode, and was affected by the emission of higher atmospheric pollutants and their precursors over southern CEC (Fig. 4), which were associated with hotspots due to open crop residual burning (Fig. 3). The daily contributions of open crop residual burning on emissions were 44–69% on 7 June which was much higher than the monthly average of 17–45% (Table 2). POC had the largest impact from open crop residual burning (69%). For simulated atmospheric pollutants, Table 4 indicates that open crop residual burning affected 12% of $O_3$, 35% of CO, 56% of EC, and 80% of OC over CEC. With regard to spatial distribution, the polluted air mass caused by open crop residual burning, whose contributions were 20–30% for $O_3$, 50–80% for CO, 60–80% for BC and OC, covered Shandong province as shown in Fig. 5 (Episode I-a). At the summit of Mount Tai, the contributions on these pollutants were 26–80%. The highly polluted air compared with the surrounding region seemed to pass directly through Mount Tai. This might have caused an elevation in these concentrations at the summit. On the possibility of a large impact from open crop residual burning on 7 June (Li et al., 2008a), this modeling study showed the magnitude of the impact.

On 12 June, as mentioned above, this model tended to underestimate $O_3$, CO, BC, and OC concentrations and these peaks were simulated one day behind the observed concentrations. Li et al. (2008a) using the data of Cao et al. (2005) for total biomass burning emissions and MODIS for their distribution, also showed the same one-day delay without underestimation. One reason for the one-day delay may be uncertainties in hotspot distributions. It should be noted that allocations of emissions from open crop residual burning relied only on hotspot data from satellites in these studies, and some which were invisible under cloud were included in the spatial distribution of these emissions and timings. and overlooked some small-scale burning. On the other hand,

the different tendencies between these modeling studies were caused both by smooth hotspots and total biomass burning emissions. Additionally, Li et al. (2008a) employed annual biomass burning emissions from Cao et al. (2005), which included emissions from biomass burning for energy. Therefore Li et al. (2008a) could not avoid double-counting for emissions from biomass used for energy because REAS also counted biofuel emissions. Instead, it is suggested that the reproduction of observed concentrations needs more emissions which are the same amount as emissions from biomass burning for energy use. The daily emissions over CEC were 46–68% of those on 7 June, which were caused by relatively lower contributions from open crop residual burning of 12–31% (Table 4). Open crop residual burning affected these concentrations which were found to be 6% of $O_3$, 16% of CO, 30% of EC, and 37% of OC over CEC. At the summit of Mount Tai, the impact of open crop residual burning was 8–65%, higher than the average in CEC. This suggested that the underestimate at the second peak for MTX2006 may have been caused by lack of emissions from open crop residual burning. Figure 5 (Episode I-b) indicates the lower contribution of open crop residual burning, which was less than 20% of the pollutants concentrations on 12 June than on 7 June (Episode I-a) over CEC. In fact, the emissions of pollutants and their precursors in the southern part of CEC on 12 June were much lower than those on 7 June (Fig. 4).

#### 4.2.2 Cleaner period between the polluted two peaks, Episode II

Relatively increased emissions due to open crop residual burning were still found over the southern part of CEC on 10 June (Fig. 4). As shown in Table 4, the contributions from open crop residual burning were still large, 26–59% of the daily emissions over CEC. Moreover, Fig. 4d also shows that CO emission in CEC on 10 June was about 1.5 times higher than that in the latter half of June without significant open crop residue burning. Open crop residual burning affected daily concentrations (6% of $O_3$, 20% of CO, 43% of EC, and 53% of OC for CEC averages), however, the impact was almost zero for those at the summit of Mount Tai. As shown in Fig. 5 (Episode II), low-pressure systems from east China to Japan with a stationary front over the west-



ACPD
9, 22103–22141, 2009



ern Pacific Ocean, brought airflow from north China and Mongolia to CEC through the upper boundary layer. The Mount Tai was just behind the strong low presser, therefore a highly polluted air mass was pushed down to the south the Mount Tai, and then the north of CEC was covered by a cleaner and drier continental air mass coming from the lateral boundary. As a result, the pushed polluted air mass containing high pollution due to open crop residual burning moved to the south of CEC, the East China Sea, and the Korean Peninsula (Fig. 5 Episode II).

#### 4.2.3 Negligible open crop residual burning period, Episode III

The last 10 days of June was not a hotspot (Fig. 3), and atmospheric pollutants and their precursors had lower emissions over CEC than those during other episodes as shown in Fig. 2c, d and Fig. 4. Table 4 also shows the negligible impact of open crop residual burning on daily emissions compared to monthly-averaged emissions. As the results demonstrate, the impact on all pollutants concentrations was almost zero over CEC including Mount Tai on 28 June (Table 4 and Fig. 5 Episode III). As shown in Fig. 5, the air quality level for EC and OC over East Asia on 28 June seemed to be much clearer than that in other episodes on 7, 10, and 12 June. This meant that open crop residual burning in CEC controlled EC and OC concentrations over East Asia during this month. The model successfully captured the daily-averaged $O_3$, EC, and OC concentrations on 28 June, although $O_3$ and OC were slightly over- and under-estimated during this period (Fig. 2). However, simulated CO was underestimated by a factor of 2–3 for the last 10 days of June (Fig. 3). According to tag analysis in their nested domain for 23–27 June (Li et al., 2008a), the contributions of $O_3$ from the south of CEC were lower compared with the polluted periods in the first half of June, and the contributions from the lateral and top boundaries nested domain were considerably high, 24.1 and 36.7%, respectively. It is highly likely that this CO underestimation was caused by underestimates of either or both CO emissions from anthropogenic sources and open biomass burning over CEC or/and CO inflow from the lateral boundary.



ACPD
9, 22103–22141, 2009



## 5 Summaries

The impact of open crop residual burning on $O_3$, CO, BC (or EC), and OC concentrations over Central East China (CEC) during the Mount Tai Experiment 2006 (MTX2006) was evaluated using the regional chemical transport model, CMAQ and daily emissions from open biomass burning.

The MTX2006 period was roughly divided into two parts: 1) polluted days with heavy open crop residual burning in the first half of June; 2) cleaner days with negligible field burning in the latter half of June. Additionally, the first half of June was defined by two high pollution episodes during 5–7 and 12–13 June, and a relatively cleaner episode during 8–10 June between the two high pollution episodes. These episodes were significantly impacted by open crop residual burning over CEC.

To evaluate the pollutants using CMAQ during the MTX2006 period in June, daily gridded emissions from open crop residual burning were developed based on a bottom-up methodology and using land cover and hotspot information from satellites.

For sensitivity model experiments on emissions from anthropogenic and open biomass burning and boundary conditions, we employed five model designs, R06YDD, R00AAM, R00YDD, R06YAD, and R06YDM using REAS for the year 2000 and 2006, daily and annual emissions for open biomass burning, and daily and monthly boundary conditions as shown in Table 1. R06YDD successfully captured the observed daily-averaged concentrations for $O_3$, CO, BC, and OC and the day-to-day variation patterns, with good correlation coefficients between the model and simulation ($r$=0.54–0.69), which was much better than those captured by R00AAM (e.g. $r$=0.00(4)–0.48). Simulated daily $O_3$ was more than 100 ppbv $O_3$ in early June and the monthly-averaged $O_3$ of 81.5 ppbv was close to the observed value of 82.5 ppbv. This was due to both improvements in anthropogenic emissions during 2006 and daily emissions from open biomass burning. The considerably large effect of daily emissions reflected monthly CO, EC, and OC concentrations and $r$ values for $O_3$, EC, and OC.

On the other hand, this model tended to underestimate CO by a factor of 2–3 and



ACPD
9, 22103–22141, 2009



BC by a factor of 2–3.5. We suggest that the underestimation of CO concentrations was affected by underestimates of emissions from both anthropogenic sources, open biomass burning and CO inflow from the lateral boundary, and underestimation of BC was largely affected by open crop residual burning over CEC. Additionally, the allocation of emissions included uncertainties in estimating the timing of open crop residual burning over CEC.

*Acknowledgements.* This work was supported by the Grants-in-Aid for Scientific Research (No. 19710024) from the Ministry of Education, the Global Environment Research Fund of the Ministry of the Environment, Japan (No. B-051, C-081, S-7), and the Joint Research Fund of Research Institute for Applied Mechanics, Kyusyu University (No. 21AO-14).

## References

Akimoto, H., Ohara, H., Kurokawa, J., and Horii N.: Verification of energy consumption in China during 1996–2003 by using satellite observational data, Atmos. Environ., 40, 7663–7667, 2006.

Allen, D., Pickering, K., and Fox-Rabinovitz, M.: Evaluation of pollutant outflow and CO sources during TRACE-P using model-calculated, aircraft-based, and Measurements of Pollution in the Troposphere (MOPITT)-derived CO concentrations, J. Geophys. Res., 109, D15S03, doi:10.1029/2003JD004250, 2004.

Andreae, M. O. and Merlet, P.: Emission of trace gases and aerosols from biomass burning, Global Biogeochem. Cy., 15, 955–966, 2001.

Arellano, A. F., Kasibhatla, P. S., Giglio, L., van der Werf, G. R., and Randerson, J. T.: Top-down estimates of global CO sources using MOPITT measurements, Geophys. Res. Lett., 31, L01104, doi:10.1029/2003GL018609, 2004.

Binkowski, F. S. and Shankar, U.: 1995The Regional Particulate Matter Model, 1. Model description and preliminary results, J. Geophys. Res. 100(D12), 26191–26209, 1995.

Byun, D. W. and Ching, J. K. S. (Eds.): Science algorithms of the EPA Models-3 community multiscale air quality (CMAQ) modeling system. NERL, Research Triangle Park, NC. EPA/600/R-99/030, 1999.





Cao, G., Zhang, X., Wang, D., and Zheng, F.: Inventory of atmospheric pollutants discharged from biomass burning in China continent, China Environ. Sci., 25, 389–393, 2005 (in Chinese).

Carmichael, G. R., Tang, Y., Kurata, G., Uno, I., Streets, D. G., Thongboonchoo, N., Woo, J.-H., Guttikunda,S., White, A., Wang, T, Blake, D. R., Atlas, E., Fried, A., Potter, B., Avery, M. A., Sachse, G. W., Sandholm, S. T., Kondo, Y., Talbot, R. W., Bandy, A. Thorton, D., and Clarke, A. D.: Evaluating regional emission estimates using the TRACE-P observations, J. Geophys. Res., 108(D21), 8810, doi:10.1029/2002JD003116, 2003.

Carter, W. P. L.: Documentation of the SAPRC-99 chemical mechanism for VOC reactivity assessment. Final report to California Air Resource Board. Contract No. 92–329 and 95–308, 2000.

Cotton, W. R., Pielke, R. A., and Walko, R. L.: RAMS 2001: Current status and future directionds, Meteorol. Atmos. Phys., 82, 5–29, 2003.

Editorial Board of China Agricultural Statistical Yearbook (EBCASY): China Agricultural Statistical Yearbook 2006, China Agricultural Press, Beijing, China, 2007 (in Chinese).

Gao, J., Wang, T., Ding, A., and Liu, C.: Observational study of ozone and carbon monoxide at the summit of mount Tai (1534 m a.s.l.) in central-eastern China, Atmos. Environ., 39, 4779–4791, 2005.

Guenther, A., Hewitt, C. N., Erickson, D., Fall, R., Geron, C., Graedel, T., Harley, P., Klinger, L., Lerdau, M., Mckay, W. A., Pierce, T., Scholes, B., Steinbrecher, R., Tallamraju, R., Taylor, J., and Zimmerman, P.:A global model of natural volatile organic compound emissions, J. Geophys. Res., 100(D5), 8873–8892, 1995.

He, Y. J., Uno, I., Wang, Z. F., Pochanart, P., Li, J., and Akimoto, H.: Significant impact of the East Asia monsoon on ozone seasonal behavior in the boundary layer of Eastern China and the west Pacific region, Atmos. Chem. Phys., 8, 7543–7555, 2008, http://www.atmos-chem-phys.net/8/7543/2008/.

Irie, H., Sudo, K., Akimoto, H., Richter, A., Burrows, J. P., Wagner, T., Wenig, M., Beirle, S., Kondo, Y., Sinyakov, V. P., and Goutail, F.: Evaluation of long-term tropospheric $NO_2$ data obtained by GOME over East Asia in 1996–2002, Geophys. Res. Lett., 32, L11810, doi:10.1029/2005GL022770, 2005.

Irie, H., Kanaya, Y., Takashima, H., Gleason, F. J., and Wang, Z.: Characterization of OMI Tropospheric $NO_2$ Measurements in East Asia Based on a Robust Validation Comparison, SOLA, 5, 117–120, 2009.





Kanaya, Y., Komazaki, Y., Pochanart, P., Liu, Y., Akimoto, H., Gao, J., Wang, T., and Wang, Z.: Mass concentrations of black carbon measured by four instruments in the middle of Central East China in June 2006, Atmos. Chem. Phys., 8, 7637–7649, 2008, http://www.atmos-chem-phys.net/8/7637/2008/.

Kanaya, Y., Pochanart, P., Liu, Y., Li, J., Tanimoto, H., Kato, S., Suthawaree, J., Inomata, S., Taketani, F., Okuzawa, K., Kawamura, K., Akimoto, H., and Wang, Z. F.: Rates and regimes of photochemical ozone production over Central East China in June 2006: a box model analysis using comprehensive measurements of ozone precursors, Atmos. Chem. Phys. Discuss., 9, 12965–12997, 2009, http://www.atmos-chem-phys-discuss.net/9/12965/2009/.

Kasibhatla, P., Arellano, A., Logan, J. A., Palmer, P. I., and Novelli, P.: Top-down estimate of a large source of atmospheric carbon monoxide associated with fuel combustion in Asia, Geophys. Res. Lett., 29, 1900, doi:10.1029/2002GL015581, 2002.

Li, J., Wang, Z., Akimoto, H., Gao, C., Pochanart, P., and Wang, X.: Modeling study of ozone seasonal cycle in lower troposphere over East Asia, J. Geophys. Res., 112, D22S25, doi:10.1029/2006JD008209, 2007.

Li, J., Wang, Z., Akimoto, H., Yamaji, K., Takigawa, M., Pochanart, P., Liu, Y., Tanimoto, H., and Kanaya, Y.: Near-ground ozone source attributions and outflow in central eastern China during MTX2006, Atmos. Chem. Phys., 8, 7335–7351, 2008a, http://www.atmos-chem-phys.net/8/7335/2008/.

Li, J., Pochanart, P., Wang, Z., Liu, Y., Yamaji, K., Takigawa, T., Kanaya, Y., and Akimoto, H.: Impact of Chemical Production and Transport on Summertime Diurnal Ozone Behavior at a Mountainous Site in North China Plain, SOLA, 4, 121–124, 2008b.

MOA/DOE Project Expert Team: Assessment of Biomass Resource Availability in China, China Environmental Science Press, Beijing, China, 1998.

Nenes, A., Pilinis, C., and Pandis, S. N.: ISORROPIA: A New Thermodynamic Model for Multiphase Multicomponent Inorganic Aerosols, Aquat. Geochem., 4, 123–152, 1998.

Ohara, T., Akimoto, H., Kurokawa, J., Horii, N., Yamaji, K., Yan, X., and Hayasaka, T.: An Asian emission inventory of anthropogenic emission sources for the period 1980–2020, Atmos. Chem. Phys., 7, 4419–4444, 2007, http://www.atmos-chem-phys.net/7/4419/2007/.

Olivier, J. G. J., Bloos, J. P. J., Berdowski, J. J. M., Visschedijk, A. J. H., and Bouwman A. F.: A 1990 global emission inventory of anthropogenic sources of carbon monoxide on 1×1 de-





gree developed in the framework of EDGAR/GEIA, Chemosphere, 1, 1–17, 1999.
Palmer, P. I., Jacob, D. J., Jones, D. B. A., Heald, C. L., Yantosca, R. M., Logan, J. A., Sachse, G. W., and Streets, D. G.: Inverting for emissions of carbon monoxide from Asia using aircraft observations over the western Pacific, J. Geophys. Res., 108(D21), 8828, doi:10.1029/2003JD003397, 2003.
Pétron, G., Granier, C., Khattatov, B., Lamarque, J., Yudin, V., Müller, J., and Gille, J.: Inverse modeling of carbon monoxide surface emissions using Climate Monitoring and Diagnostics Laboratory network observations, J. Geophys. Res., 107(D24), 4761, doi:10.1029/2001JD001305, 2002.
Pielke, R. A., Cotton, W. R., Walko, R. L., Tremback, C. J., Lyons, W. A., Grasso, L. D., Nicholls, M. E., Moran, M. D., Wesley, D. A., Lee, T. J., and Copeland, J. H.: A comprehensive meteorological modeling system–RAMS, Meteorol. Atmos. Phys., 49, 69–91, 1992.
Richter, A., Burrows, J. P., Nüß, H., Granier, C., and Niemeier, U.: Increase in tropospheric nitrogen dioxide over China observed from space, Nature, 437, 129–132, doi:10.1038/nature04092, 2005.
Schell, B., Ackermann, I. J., Hass, H., Binkowski, F. S., and Ebel, A.: Modeling the formation of secondary organic aerosol within a comprehensive air quality model system. J. Geophys. Res., 106(D22), 28275–28293, 2001.
Song, J. B., Survey and analysis of crop residue resources and quality in Zhejing Province, Soil and Fertilizer, 2, 23–24, 1995 (in Chinese).
Streets, D. G. and Waldhoff, S. T.: Present and future emissions of air pollutants in China: $SO_2$, $NO_x$ and CO, Atmos. Environ., 34, 363–374, 2000a.
Streets, D. G., Tsai, N. Y., Akimoto, H., and Oka, K.: Sulfur dioxide emissions in Asia in the period 1985–1997, Atmos. Environ., 34, 4413–4424, 2000b.
Streets, D. G., Bond, T. C., Carmichael, G. R., Fernandes, S. D., Fu, Q., He, D., Klimont, Z., Nelson, S. M., Tsai, N. Y., Wang, M. Q., Woo, J.-H., and Yarber, K. F.: An inventory of gaseous and primary aerosol emissions in Asia in the year 2000, J. Geophys. Res., 108, 8809, doi:10.1029/2002JD003093, 2003.
Streets, D. G., Zhang, Q., Wang, L., He, K., Hao, J., Wu, Y.,Tang, Y., and Carmichael, G. R.: Revisiting China's CO emissions after the Transport and Chemical Evolution over the Pacific (TRACE-P) mission: synthesis of inventories, atmospheric modeling, and observations, J. Geophys. Res., 111, D14306, doi:10.1029/2006JD007118, 2006.
Sudo, K., Takahashi, M., Kurokawa, J., and Akimoto, H.: CHASER: a global chemical

model of the troposphere – 1. Model description, J. Geophys. Res., 107(D17), 4339, doi:10.1029/2001JD001113, 2002.
Sudo, K. and Akimoto, H.: Global source attribution of tropospheric ozone: Long-range transport from various source regions, J. Geophys. Res., 112, D12302, doi:10.1029/2006JD007992, 2007.
Tan, Q., Chameides, W. L., Streets, D., Wang, T., Xu, J., Bergin, M., and Woo, J.: An evaluation of TRACE-P emission inventories from China using a regional model and chemical measurements, J. Geophys. Res., 109, D22305, doi:10.1029/2004JD005071, 2004.
Turpin B. J. and Lim H.-J.: Species contributions to PM2.5 mass concentrations: revisiting common assumptions for estimating organic mass, Aerosol Sci. Tech., 35, 602–610, 2001.
Uno, I., He, Y., Ohara, T., Yamaji, K., Kurokawa, J.-I., Katayama, M., Wang, Z., Noguchi, K., Hayashida, S., Richter, A., and Burrows, J. P.: Systematic analysis of interannual and seasonal variations of model-simulated tropospheric NO2 in Asia and comparison with GOME-satellite data, Atmos. Chem. Phys., 7, 1671–1681, 2007, http://www.atmos-chem-phys.net/7/1671/2007/.
White, W. H. and Roberts, P. T.: On the nature and origins of visibility-reducing aerosols in the Los Angeles Air Basin, Atmos. Environ., 11, 803–812, 1977.
Yamaji, K., Ohara, T., and Akimoto, H.: A country-specific, high resolution emission inventory for methane from livestock in Asia in 2000, Atmos. Environ., 37, 4393–4406, 2003.
Yamaji, K., Ohara, T., and Akimoto, H.: Regional-specific emission inventory for $NH_3$, $N_2O$, and $CH_4$ via animal farming in South, Southeast, and East Asia, Atmos. Environ., 38, 7111–7121, 2004.
Yamaji, K., Ohara, T., Uno, I., Tanimoto, H., Kurokawa, J., and Akimoto, H.: Analysis of the seasonal variation of ozone in the boundary layer in East Asia using the Community Multi-scale Air Quality model: What controls surface ozone levels over Japan?, Atmos. Environ., 40, 1856–1868, 2006.
Yamaji, K., Ohara, T., Uno, I., Kurokawa, J., Pochanart, P., and Akimoto, H.: Future prediction of surface ozone over east Asia using models-3 community multiscale air quality modeling system and regional emission inventory in Asia, J. Geophys. Res., 113, D08306, doi:10.1029/2007JD008663, 2008.
Yan, X., Akimoto, H., and Ohara, T.: Estimation of nitrous oxide, nitric oxide, and ammonia emissions from croplands in East, Southeast, and South Asia, Glob. Change Biol., 9, 1080–1096, 2003.



ACPD
9, 22103–22141, 2009



Yan, X., Ohara, T., and Akimoto, H.: Bottom-up estimate of biomass burning in mainland China, Atmos. Environ., 40, 5262–5273, 2006.
Yang, S. J.: Emphasizing the use of crop residue as energy source, Rural Energy, 58, 18–19, 1994 (in Chinese).
Zhang, M. G., Uno, I., Sugata, S., Wang, Z. F., Byun, D., and Akimoto, H.: Numerical study of boundary layer ozone transport and photochemical production in east Asia in the wintertime. Geophys. Res. Lett. 29, 1545, doi:10.1029/2001GL014368, 2002.



ACPD
9, 22103–22141, 2009



**Table 1.** Sensitivity model experiment designs.

| | Emissions | | Boundary condition |
|---|---|---|---|
| | Anthropogenic sources | Open biomass burning | |
| R06YDD | REAS[a], year 2006 (estimated) | This study[b], year 2006 (daily) | CHASER[d], year 2006 (daily) |
| R00AAM | REAS, year 2000 (bottom up) | ACESS[c], year 2001 (annual) | CHASER, climate (monthly) |
| R00YDD | REAS, year 2000 (bottom up) | This study, year 2006 (daily) | CHASER, year 2006 (daily) |
| R06YAD | REAS, year 2006 (estimated) | This study, year 2006 (annual) | CHASER, year 2006 (daily) |
| R06YDM | REAS, year 2006 (estimated) | This study, year 2006 (daily) | CHASER, climate (monthly) |

[a]Regional emission inventory in Asia (Ohara et al., 2007), [b]Using a bottom-up methodology by Yan et al. (2006) for annual emissions estimation and the MODIS (MOerate resolution Imaging Spectroradiometer) fire database for the spatial and temporal allocations, [c]ACE-Asia and TRACE-P Modeling and Emission Support System (Streets et al., 2003), [d]Chemical AGCM for Study of Atmospheric Environment and Radiative forcing (Sudo et al., 2002). Here, "RyyABC" means that: (Ryy) the REAS base year, 2000 or 2006 (R00 or R06), (A) the methodology to estimate emissions from open crop residual burning, ACESS (Streets et al., 2003) or Yan et al. (2006) (A or Y), (B) the time resolution of emissions from open crop residual burning, daily or annually (D or A), and (C) the time resolution of boundary condition (D or M).





**Table 2.** Emissions from open biomass burning in China (Gg species $yr^{-1}$).

| | Year | $NO_x$ (as $NO_2$) | $SO_2$ | CO | $NH_3$ | EC | OC | NMVOC |
|---|---|---|---|---|---|---|---|---|
| | | | | Field burning of crop residue | | | | |
| This study | 2006 | 528 | 55 | 12 673 | 179 | 95 | 455 | 2163 |
| Yan et al. [2006] | 2000 | 468 | 49 | 11 231 | 159 | 84 | 403 | 1917 |
| ACESS[a] | 2001 | 403 | 42 | 9691 | 137 | 73 | 348 | 1654 |
| | | | | Forest and grassland fires | | | | |
| Yan et al. [2006][b] | 2000 | 266 | 53 | 5791 | 77 | 31 | 486 | 1160 |
| ACESS[a] | 2001 | 413 | 40 | 6051 | 89 | 40 | 380 | 1037 |

[a] Streets et al. (2003) (available at http://www.cgrer.uiowa.edu/ACESS/acess_index.htm),
[b] These emissions from forest and grassland fires were used in this study.



ACPD
9, 22103–22141, 2009



**Table 3.** Comparisons of daily simulated and observed atmospheric pollutants at the summit of Mount Tai in June 2006.

| Sensitivity model experiment designa | | | R06YDD | R00AAM | R00YDD | R06YAD | R06YDM |
|---|---|---|---|---|---|---|---|
| | Observation ($n$)[b] | | | | Mounthly mean | | |
| $O_3$ (ppbv) | 82.5 | **(27)** | 81.5 | 69.6 | 75.8 | 76.0 | 84.7 |
| CO (ppbv) | 567.7 | **(26)** | 313.1 | 192.3 | 311.8 | 241.5 | 309.5 |
| BC or EC ($\mu g\,m^{-3}$) | | | | | | | |
| (ECOC, EC, PM1) | 2.97 | **(13)** | 1.52 | 0.65 | 1.62 | 0.80 | 1.47 |
| (MAAP ,BC, PM2.5) | 3.83 | **(30)** | 1.27 | 0.60 | 1.28 | 0.81 | 1.29 |
| (MAAP, BC, PM1) | 3.45 | **(30)** | 1.27 | 0.60 | 1.28 | 0.81 | 1.29 |
| OC, PM1 ($\mu g\,m^{-3}$) | 9.14 | **(16)** | 6.61 | 1.67 | 7.24 | 2.36 | 6.66 |
| | | | | | Correlation coefficient ($r$) | | |
| $O_3$ | | **(27)** | 0.61 | 0.48 | 0.68 | 0.35 | 0.64 |
| CO | | **(26)** | 0.54 | 0.35 | 0.49 | 0.54 | 0.46 |
| BC or EC | | | | | | | |
| (ECOC, EC, PM1) | | **(13)** | 0.66 | 0.19 | 0.62 | 0.21 | 0.66 |
| (MAAP, BC, PM2.5) | | **(30)** | 0.63 | 0.06 | 0.58 | 0.24 | 0.59 |
| (MAAP, BC, PM1) | | **(30)** | 0.65 | 0.03 | 0.62 | 0.24 | 0.62 |
| OC, PM1 | | **(16)** | 0.63 | 0.00 | 0.61 | 0.34 | 0.55 |

[a] see Table 1, [b] $n$ are the numbers of samples.



ACPD
9, 22103–22141, 2009



**Table 4.** Daily emissions from CEC and simulated $O_3$, CO, EC, and OC[a] concentrations at CEC and the summit of Mount Tai for the Episodes (I-a, II, I-b,III) and monthly mean in June.

| | | Episode I-a 7 June | | Episode II 10 June | | Episode I-b 12 June | | Episode III 28 June | | monthly mean | |
|---|---|---|---|---|---|---|---|---|---|---|---|
| | | | | | | Emissions at CEC[c] | | | | | |
| $NO_x$ | kmol $s^{-1}$ (%)[b] | 9.4 | (44) | 6.4 | (26) | 5.4 | (12) | 4.5 | (2) | 5.6 | (17) |
| CO | kmol $s^{-1}$ (%) | 270.1 | (60) | 152.4 | (42) | 115.2 | (22) | 78.7 | (4) | 124.3 | (30) |
| PEC | kg $s^{-1}$ (%) | 54.2 | (63) | 29.9 | (45) | 21.8 | (24) | 14.7 | (4) | 24.0 | (33) |
| POC | kg $s^{-1}$ (%) | 239.2 | (69) | 111.1 | (59) | 80.3 | (31) | 30.5 | (9) | 83.9 | (45) |
| | | | | | | Concentrations at CEC[d] | | | | | |
| $O_3$ | ppmv (%) | 71.9 | (12) | 50.8 | (6) | 73.6 | (6) | 65.7 | (0) | 72.4 | (5) |
| CO | ppmv (%) | 376.3 | (35) | 222.2 | (20) | 258.1 | (16) | 218.0 | (1) | 294.3 | (17) |
| EC | $\mu$g $m^{-3}$ (%) | 1.81 | (56) | 0.77 | (43) | 1.00 | (30) | 0.65 | (2) | 1.22 | (30) |
| OC | $\mu$g $m^{-3}$ (%) | 8.30 | (80) | 3.03 | (53) | 4.01 | (37) | 1.89 | (3) | 4.90 | (37) |
| | | | | | | Concentrations at the summit of Mount Tai[e] | | | | | |
| $O_3$ | ppmv (%) | 106.0 | (26) | 43.5 | (0) | 77.4 | (8) | 80.4 | (0) | 81.2 | (6) |
| CO | ppmv (%) | 678.3 | (62) | 174.3 | (0) | 297.5 | (33) | 236.9 | (0) | 301.4 | (22) |
| EC | $\mu$g $m^{-3}$ (%) | 3.93 | (79) | 0.38 | (0) | 1.23 | (58) | 0.65 | (1) | 1.27 | (37) |
| OC | $\mu$g $m^{-3}$ (%) | 18.81 | (80) | 0.73 | (3) | 5.52 | (65) | 1.82 | (1) | 5.23 | (44) |

[a] OC includes secondary organic molecule. [b] Percent (%) signifys impacts from open crop residual burning. [c] Emissions from CEC (Central East China) shown in Fig. 1. [d] Simulated concentrations in the near-ground (<≈1000-m altitude) over CEC. [e] Simulated concentrations at the summit of Mount Tai (≈1000-m altitude).



ACPD
9, 22103–22141, 2009



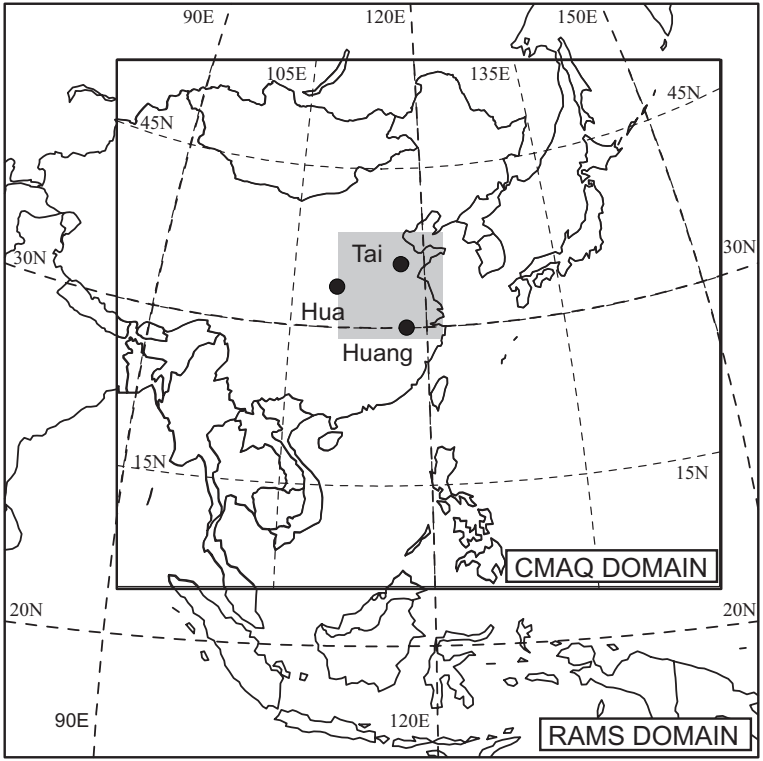


**Fig. 1.** Model domains for CMAQ (inside) and RAMS (outside) simulations. Tai (Mount Tai) (36.25° N, 117.10° E, 1533 m a.s.l.), Hua (Mount Hua) (34.49° N, 110.09° E, 2064 m a.s.l.), Huang (Mount Huang) (30.13° N, 118.15° E, 1836 m a.s.l.) are plotted. The domain with a dark gray shadow is defined as Central Eastern China (CEC).



ACPD
9, 22103–22141, 2009



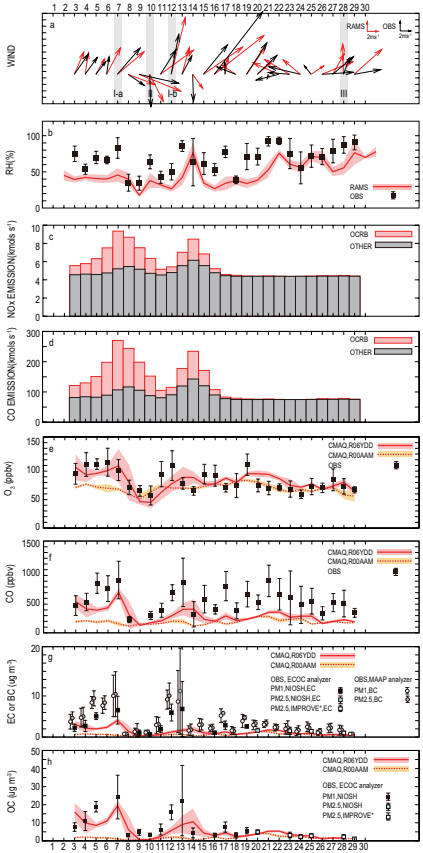


**Fig. 2.** Daily values of simulated and observed meteorological conditions at the summit of Mount Tai, $NO_x$ and CO emissions over CEC, and simulated and observed chemical concentrations at the summit of Mount Tai, in June 2006: **(a)** simulated and observed wind fields; **(b)** simulated and observed relative humidity (RH) with SD ($\pm 1\sigma$) (simulated: shadow, observed: bars); **(c)** daily $NO_x$ emissions, OCRB (emissions from open crop residual burning) and OTHR (emissions from the other sources); **(d)** daily CO emissions; **(e)** daily simulated and observed CO with SD ($\pm 1\sigma$) (simulated: shadows, observed: bars), CMAQ R06YDD, using REAS2006, daily biomass burning emissions, and daily boundary conditions and CMAQ R00AAMD, using REAS2000, annual biomass burning emissions, and monthly boundary conditions (see Table1); **(f)** daily simulated and observed $O_3$ with SD ($\pm 1\sigma$); **(g)** daily simulated EC and observed EC or BC using ECOC analyzer (Sunset Laboratory) and MAAP analyzer (5012 MAAP, Thermo) (Kanaya et al., 2008) with SD ($\pm 1\sigma$); **(h)** daily simulated and observed OC with SD ($\pm 1\sigma$).



ACPD
9, 22103–22141, 2009



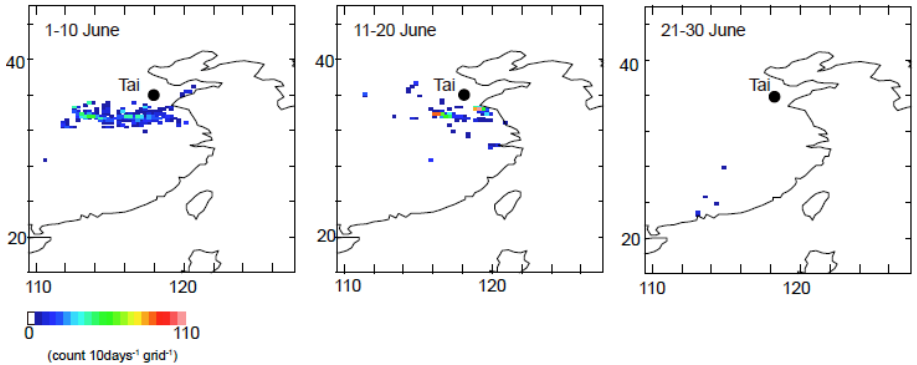


**Fig. 3.** Hotspot numbers (count 10 days$^{-1}$ grid$^{-1}$) observed by Aqua/Terra MODIS (MOerate resolution Imaging Spectroradiometer, http://webmodis.iis.u-tokyo.ac.jp/) for 1–10, 11–20, 21–30 June 2006.



ACPD
9, 22103–22141, 2009



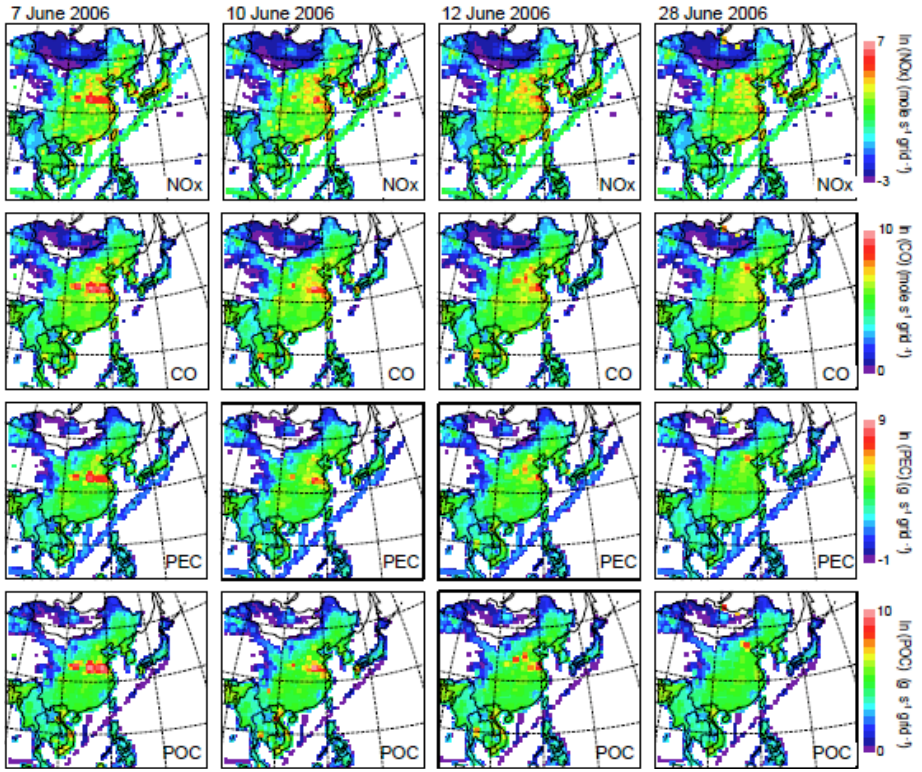


**Fig. 4.** Spatial distributions of $NO_x$, CO, PEC, and POC emissions from all sources on 7, 10, 12, and 28 June 2006.



ACPD

9, 22103–22141, 2009



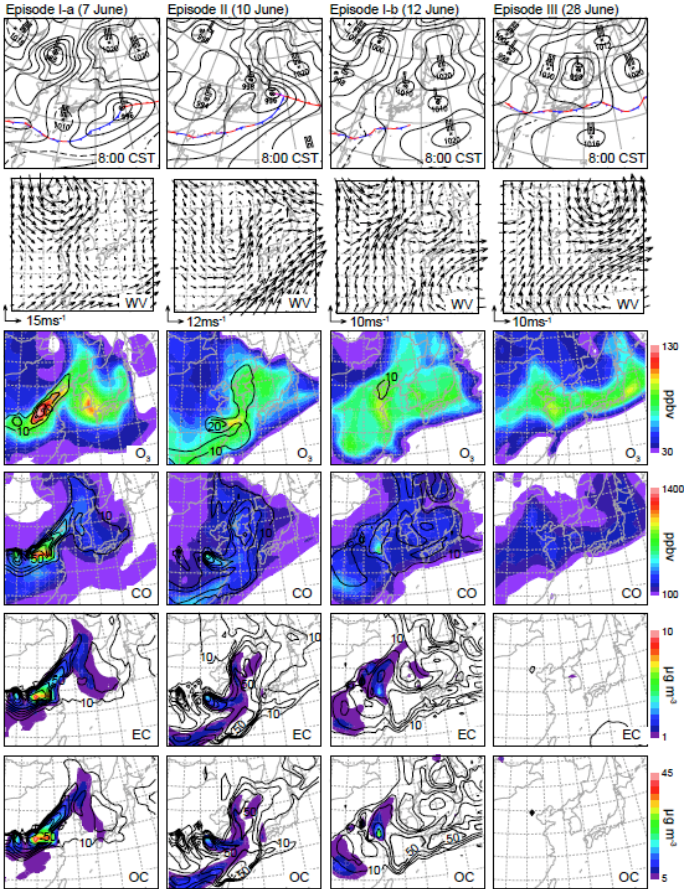


**Fig. 5.** Spatial distributions of surface meteorological fields and simulated atmospheric concentrations for Episode I-a on 7 June, Episode I-b on 12 June, Episode II on 10 June, and Episode III on 28 June 2006 over East Asia. Top four panels: The surface weather chart at 8:00 CST/0:00 UTC for each day is also shown on top line from Japan Meteorological Agency (http://www.data.jma.go.jp/fcd/yoho/hibiten/index.html). The second four panels: Simulated wind fields below ≈1000-m altitude. Bottom panels: $O_3$, CO, EC, and OC concentrations (colors), <≈1000-m altitude. Contours are impacts from open crop residual burning in China (%): thick solid lines mean each 20% of $O_3$ and 50% for CO, BC, and OC; thin solid lines mean each 10% of $O_3$, CO, BC, and OC. The impacts are calculated from the differences between R06YDD and the other simulation without emissions from open crop residual burning for China.



ACPD
9, 22103–22141, 2009